PAPER

Check for updates

Synthesis of amine derivatives from furoin and furil over a Ru/Al$_2$O$_3$ catalyst†

Li Gao,[a] Massimo Delle Piane, [iD] ‡[b] Marta Corno, [iD] [c] Fan Jiang,[a] Robert Raja [iD] [d] and M. Pera-Titus [iD] *[ae]

The direct/reductive amination of carbohydrate-based furoin and furil with NH$_3$/H$_2$ was investigated to access amine derivatives. In the sole presence of NH$_3$, cyclic amines, *i.e.* 2,3,5,6-tetra(furan-2-yl)pyrazine and 2,2′-bipyridine-3,3′-diol, were generated as the main products from furoin and furil, respectively. Over Ru/Al$_2$O$_3$ under NH$_3$/H$_2$, 2-amino-1,2-di(furan-2-yl)ethan-1-ol (*i.e.* alcohol–amine) was generated as the main product with 47% yield at 140 °C for 2 h starting from furoin. The catalyst could be recycled for at least three consecutive runs. An alcohol–imine was the main intermediate that underwent tautomerization to alcohol–enamine/keto–amine leading to cyclic by-products by self-condensation. DFT calculations, complementing the experimental observations, provided detailed molecular-level insight into the reactivity of the alcohol–imine intermediate. Its preferential adsorption on Ru centers *via* the NH group, with the OH group pointing away from the surface, was found to direct its hydrogenation towards the alcohol–amine as main product. By combining Ru/Al$_2$O$_3$ and a silica-anchored N-heterocyclic carbene (NHC) catalyst, the alcohol-amine could be accessed with 42% overall yield in a single reactor.

Introduction

Furfural (FF) is a cheap commercial platform molecule (1.0–1.2€ per kg) that can be prepared at a large scale by dehydration of carbohydrates (>200 kT per year).[1] FF can be used as a building block for accessing a variety of products and intermediates.[1c,2] In particular, FF can be converted into amines by reductive amination, which are valuable intermediates to manufacture polymers, surfactants, biologically active molecules and pharmaceuticals (*e.g.*, furosemide).[3] The synthesis of furfurylamines can be conducted from FF and 5-hydroxymethylfurfural (HMF) by direct/reductive amination over homogeneous and heterogeneous catalysts.[4] Also, secondary and tertiary tetrahydrofurfurylamines can be

accessed with high yield (>90%) from FF over Pd/Al$_2$O$_3$ at room temperature and 1 bar H$_2$.[5]

An upgrading process of FF comprises C–C bond coupling and amination. In this view, it is desirable to design multistep processes with a high degree of intensification and high activity/selectivity to the desired amines. One-pot reactions have been reported for the synthesis of furan- and THF-derived amines combining an aldol condensation reaction of FF with ketones, followed by reductive amination with NH$_3$ and H$_2$, over a mixture of Amberlyst-26 (A26) and Ru/C or Pd/Al$_2$O$_3$ catalysts.[6] For example, using Pd/Al$_2$O$_3$ as a catalyst and H$_2$ (2.0 MPa) as a reductant, 98% overall yield of THF–amine was achieved at 120 °C after 20 h.[6b]

Benzoin condensation is a C–C coupling reaction that can promote the self-condensation of aldehydes using nucleophiles such as cyanides or N-heterocyclic carbenes (NHC) as catalysts.[7] FF and HMF can self-condense towards 5,5′-dihydroxymethylfuroin (DHMF) derivatives using NHC organocatalysts.[8] The reaction mechanism operates *via* umpolung condensation as proposed by Breslow.[9] In particular, benz-imidazolium (bim) salts with one/two long-chain aliphatic substituents at the N-atoms in the imidazole ring are active catalysts for the reaction.[10] Bim catalysts have been supported over silica and polymers with controlled mesoporosity, affording recyclable heterogeneous catalysts.[11] In the presence of a base (*e.g.*, 1,8-diazabicylo-[5.4.0]undec-7-ene, DBU), supported bim catalysts can catalyze the self-condensation of FF into furoin with 96–99% yield over three

[a] *Eco-Efficient Products and Processes Laboratory (E2P2L), UMI 3464 CNRS-Solvay, 3966 Jin Du Road, Xin Zhuang Ind. Zone, 201108 Shanghai, China*

[b] *Faculty of Production Engineering and Bremen Center for Computational Materials Science, University of Bremen, Am Fallturm 1, 28359 Bremen, Germany*

[c] *Department of Chemistry, University of Torino, Via P. Giuria 7, 10125 Torino, Italy*

[d] *School of Chemistry, University of Southampton, Highfield campus, Southampton SO171BJ, UK*

[e] *Cardiff Catalysis Institute, School of Chemistry, Cardiff University, Main Building, Park Place, Cardiff CF10 3AT, UK. E-mail: peratitusm@cardiff.ac.uk*

† Electronic supplementary information (ESI) available. See DOI: https://doi.org/10.1039/d3cy01605f

‡ Current address: Department of Applied Science and Technology, Politecnico di Torino, Corso Duca degli Abruzzi 24, 10129 Torino, Italy.

This journal is © The Royal Society of Chemistry 2024

Catal. Sci. Technol., 2024, **14**, 2593–2599 | **2593**

consecutive runs. Sequential reactions have been developed encompassing furoin derivatives targeting the synthesis of branched alkanes. Furoin/furil intermediates derived from FF can be hydrogenated towards THF-derivatives and subjected to ring opening by hydrodeoxygenation over Pd/C + La(OTf)$_3$/ Eu(OTf)$_3$ catalysts, accessing C$_{10}$–C$_{12}$ diesel fuels.[8b,12] Furoin/ furil intermediates have also been employed to prepare C$_{12}$ biofuels by subsequent esterification and etherification reactions.[13]
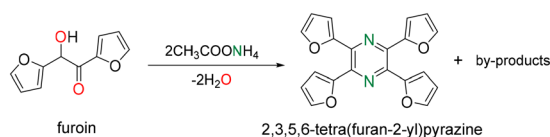
Herein we investigated the direct/reductive amination of furoin and furil with NH$_3$/H$_2$ over 5% Ru/Al$_2$O$_3$. DFT calculations were implemented to rationalize the nature and stability of surface species on Ru(0001) in the presence of adsorbed NH$_3$ and ad-H, as well as the formation of 2-amino-1,2-di(furan-2-yl)ethan-1-ol (*i.e.* alcohol–amine) as main product and the alcohol–imine and its tautomers leading to cyclic by-products. We also engineered a single-reactor tandem process by combining silica-supported bim to catalyze benzoin condensation (C–C coupling), and 5% Ru/ Al$_2$O$_3$ to catalyze reductive amination, to access furoin alcohol–amine starting from FF.

Results and discussion

Catalyst-free conversion of furoin/furil under NH$_3$

Furoin was first reacted with both NH$_3$ and ammonium acetate as an NH$_3$ surrogate in *N,N*-dimethylformamide (DMF). 2,3,5,6-Tetra(furan-2-yl)pyrazine is generated as the main product at a temperature higher than 130 °C (Scheme 1), which is in accordance with an earlier report.[14] The yield is about 15–18% at full furoin conversion by reacting furoin at 140 °C for 4 h, using 0.06 g of furoin, 6 mL of DMF and 1 g of ammonium acetate (or 0.22 g NH$_3$). A myriad of minor products are generated with low yield (<5%), including 2-amino-1,2-di(furan-2-yl)ethan-1-ol. The easier operation and higher solubility of ammonium acetate as a masked NH$_3$ reagent compared to gas NH$_3$ prompted us to use this reagent in the forthcoming experiments.

We next explored the effect of the operation variables on the yield of 2,3,5,6-tetra(furan-2-yl)pyrazine at 140 °C for 4 h. Among the solvents tested, DMF, THF and 2-methyl-THF afford a yield of 18–21% (Table S1†). The reaction does not proceed in water most likely due to the poor solubility of furoin. We further studied the effect of the temperature using THF for 3 h reaction while keeping the other reaction conditions unchanged (Table S2†). The yield of 2,3,5,6-tetra(furan-2-yl)pyrazine increases monotonously in the range of 130–160 °C up to 30% at full conversion. The highest yield

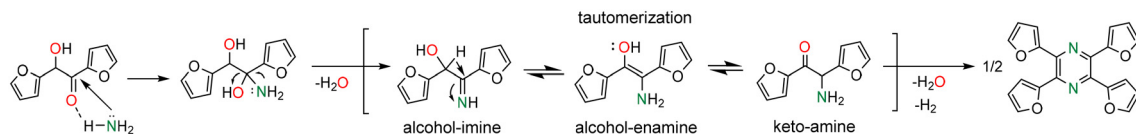**Scheme 1** Catalyst-free furoin amination with NH$_3$/ammonium acetate.

(30%) occurs for an ammonium acetate loading above 0.1 g at 160 °C in THF (Table S3†). The yield of 2,3,5,6-tetra(furan-2-yl)pyrazine reaches 44% at 160 °C for 3 h using dry THF and dry ammonium acetate (Table S4†).

A possible reaction mechanism for 2,3,5,6-tetra(furan-2-yl) pyrazine formation by reaction of furoin with ammonium acetate/NH$_3$ is depicted in Scheme 2. The first step consists of the nucleophilic attack of NH$_3$ to the carbonyl group of furoin to generate an alcohol–imine intermediate with concomitant release of one water molecule. This intermediate can undergo tautomerization to alcohol–enamine/keto–amine by-products (*m/z* = 191) that can be hardly distinguished by GC-MS. The self-condensation of the keto–amine, followed by dehydrogenation, results in 2,3,5,6-tetra(furan-2-yl)pyrazine.

Next, we reacted furil with NH$_3$ in DMF. 2,2′-Bipyridine-3,3′-diol is generated as the main product with a yield of 22% at 170 °C after 4 h at full furil conversion (Scheme 3, Table S5†). A variety of by-products are generated with low yield (<5%), including 2-amino-1,2-di(furan-2-yl)ethan-1-ol and 1,2-di(furan-2-yl)ethane-1,2-diamine (*i.e.* diamine). The yield of 2,2′-bipyridine-3,3′-diol increases to 36% at 180 °C, but decreases further to 24% at 200 °C (Table S6†). This observation suggests partial product/substrate decomposition at higher temperature. The formation of 2,2′-bipyridine-3,3′-diol can be rationalized on the basis of the mechanism depicted in Scheme 4. Furil reacts fast with NH$_3$ generating a diimine intermediate. This intermediate is unstable and may be easily activated by a proton in solution favoring ring activation and intramolecular rearrangement leading to pyridine rings. The diimine intermediate can also suffer from reversible polymerization, as earlier observed for diformylfuran upon exposure to NH$_3$.[15]

Furoin and furil amination in the presence of a catalyst

With the results above, we studied the reductive amination of furoin and furil with NH$_3$ and H$_2$. The catalytic tests were first conducted using furoin at 80 °C and 100 °C in DMF over 5% Pd/Al$_2$O$_3$ and 5% Ru/Al$_2$O$_3$ catalysts (Fig. S1† and 1). Pd/ Al$_2$O$_3$ provides a broad distribution of products, especially at lower temperature (Fig. 1A). In contrast, the alcohol–amine is formed as the main product over Ru/Al$_2$O$_3$ (Fig. 1B), as confirmed by GC-MS and ^{1}H NMR (presence of two doublets centered at 4.7 ppm and 5.4 ppm) (Fig. S2†). The alcohol–imine and its possible tautomers (keto–amine, alcohol–enamine), and the keto–imine, appear as the main by-products. The detection of the keto–imine suggests the formation of furil from furoin dehydrogenation along the reaction despite the presence of H$_2$ in the reaction medium. Indeed, we confirmed that furil can be generated at room temperature under neat conditions (*i.e.* without NH$_3$/H$_2$) (Fig. 1C). Additional peaks are observed at higher temperature (not shown) that can be attributed to cyclic by-products, especially 2,3,5,6-tetra(furan-2-yl)pyrazine, and minor formation of oligomers.

2594 | *Catal. Sci. Technol.*, 2024, **14**, 2593–2599

This journal is © The Royal Society of Chemistry 2024

Scheme 2 Proposed mechanism for 2,3,5,6-tetra(furan-2-yl)pyrazine formation from the reaction of furoin with ammonium acetate/NH₃.

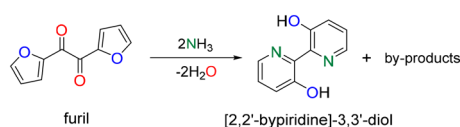We measured the yield of alcohol–amine from furoin amination over 5% Pd/Al₂O₃, 5% Ru/Al₂O₃, 5% Rh/Al₂O₃ and 5% Pt/Al₂O₃, at 160 °C for 2 h (Table 1). The first three catalysts exhibit poor yield (up to 28%) (entries 1–3), whereas the yield over 5% Ru/Al₂O₃ is the highest (40%) (entry 7) at full furoin conversion. The yield of alcohol–amine is poorly affected by the Ru loading (entries 4–6) and the type of support (*i.e.* alumina, silica, carbon) at the same Ru loading (5 wt%) (entries 7–9). The alcohol–imine and its tautomers are generated as the main by-products, as well as 2,3,5,6-tetra(furan-2-yl)pyrazine (not quantified).

The yield of alcohol–amine increases with the temperature in the range of 80–140 °C at 4.0 MPa H₂ pressure with a maximum value of 47%, but decreases slightly further to 40% at 160 °C that we attribute to the formation of oligomers (Fig. 2). The yield of alcohol–amine also increases with the H₂ pressure in the range of 0.5–4.0 MPa at constant temperature (160 °C) and keeps unchanged beyond 4.0 MPa (Fig. 3). The alcohol–imine (and possible tautomers) is generated as the main by-product, which can be further hydrogenated to the alcohol–amine product and generate 2,3,5,6-tetra(furan-2-yl)pyrazine and oligomers that were not quantified. However, the keto–imine, which is generated at 80 and 100 °C, vanishes at higher temperature. The catalyst is robust under reaction conditions, and can be reused for three consecutive catalytic runs with a yield of alcohol–amine in the range of 40–45% (Fig. 4).

We also studied the reductive amination of furil with NH₃ and H₂ over Ru/Al₂O₃. As in the case of furoin, the alcohol–amine is generated as the main product with 34% yield together with the diimine and 2,2′-bipyridine-3,3′-diol as the main by-products, as well as oligomers. Diamines are generated with less than 5% yield.

Understanding furoin amination over 5% Ru/Al₂O₃

The results above point out the preferential formation of the alcohol–amine product over Ru/Al₂O₃ at 140 °C and 2.0 MPa H₂ pressure starting from furoin, with ketone–amine/alcohol–imine being the main intermediates. To rationalize the formation of the alcohol–amine and cyclic by-products,
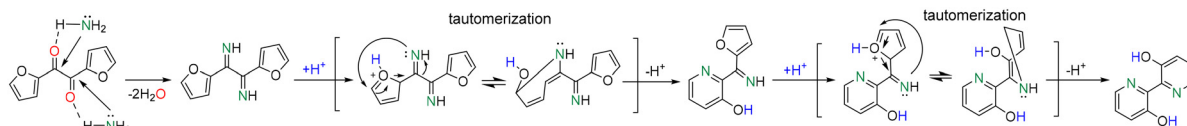
we computed the adsorption configurations and energies of the reactants (furoin, furil), end products (alcohol–amine, diamine) and possible intermediates (alcohol–imine + tautomers, diimine). The calculations were carried out both on a bare reduced Ru(0001) surface and on a reduced Ru(0001) surface covered with NH₃ and ad-H, at the DFT-PBE level (see the ESI† for computational details).

Table 2 lists the adsorption energies for the optimized configurations of the reactants, products and intermediates on bare and ad-H/NH₃-covered Ru(0001). For adsorbed furoin (entries 1–4), four configurations were probed on the bare Ru(0001) interacting *via* (Scheme 5): i) C=O group, ii) OH group, iii) both C=O and OH groups, and iv) furan rings. The most stable configuration, *i.e.* iii), corresponds to a bidentate binding mode with C=O showing the shortest Ru–O distance. The adsorption energy on bare Ru(0001) (-156 kJ mol^{-1}) (entry 4) is almost twice the sum of the energies for monodentate adsorption *via* C=O (i) and OH (ii) groups, *i.e.* -59 and -37 kJ mol^{-1}, respectively (entries 1–2). No stable configuration occurs *via* furan rings as inferred from the positive adsorption energy ($+14$ kJ mol^{-1}) (entry 3).

Few studies describe the atomistic details of H₂ and NH₃ co-adsorption on Ru(0001).[16] H₂ and NH₃ are known to occupy different sites on the Ru(0001) surface, so that ad-H atoms can influence the adsorption pattern of NH₃ on Ru(0001).[16] Since ad-H atoms occupy mainly fcc sites,[17] we simulated the dissociative H₂ chemisorption on fcc sites and NH₃ adsorption on adjacent top sites. First, we simulated a full monolayer of ad-H on fcc sites without NH₃ (Scheme 5a1). The adsorption energy is -111 kJ mol^{-1} and keeps unchanged when implicit solvation by DMF is included (-112 kJ mol^{-1}). Next, we simulated NH₃ chemisorption on only 25% of available top sites to take into account steric constraints (Scheme 5a2). Also, we assumed that no NH₃ dissociation occurs at the reaction temperature (up to 160 °C) given its high activation energy (>100 kJ mol^{-1}),[18] and that adsorbed NH₃ is known to keep undissociated in the presence of ad-H species below 170 °C.[17,19] The adsorption energy of NH₃ is -75 kJ mol^{-1} with a limited stabilizing effect of DMF (-5 kJ mol^{-1}), which agrees well with an earlier report.[20] The average N–Ru distance is 2.2 Å that is similar to the distance measured for diamine and diimine derivatives. We also computed H₂ and NH₃ co-adsorption on Ru(0001) (Scheme 5a3). After geometry optimization, half of ad-H atoms move to neighboring hcp sites with a hexagonal arrangement around each adsorbed NH₃ molecule. The adsorption energy is -101 kJ mol^{-1} (-104 kJ mol^{-1} in DMF).

Using the optimized NH₃- and ad-H-covered Ru(0001) surface, we simulated the adsorption of furoin/furil, products

Scheme 3 Catalyst-free furil amination with NH₃.

Scheme 4 Possible mechanism for 2,2′-bipyridine-3,3′-diol formation from the reaction of furil with NH_3.

Fig. 1 Representative GC plots for furoin amination with NH_3 and H_2 over (A) 5% Pd/Al_2O_3, (B) 5% Ru/Al_2O_3, and (C) neat conditions (RT) with neither NH_3 nor H_2. Reaction conditions: furoin (0.12 g, 0.625 mmol), catalyst (24 mg), NH_3 (0.7 g), DMF (2 g), 100 °C, 4.0 MPa H_2, 2 h. The catalysts were pre-reduced at 200 °C before the reaction.

and intermediates, and recomputed the adsorption energies (Scheme 5b–g, Table 2). As a rule, although the adsorption energies can show variations when different NH_3 and ad-H coverages are considered, the primary effect on the relative stability of the different species and their orientation is expected to be poorly affected.[21] With these considerations, all adsorption energies are lower on the NH_3- and ad-H-covered Ru(0001) surface than on bare Ru(0001). However, the relative stability between furoin, diamine and diimine is preserved. Furil exhibits stronger adsorption than furoin (-107 kJ mol^{-1} *vs.* -74 kJ mol^{-1}, compare entries 5 and 4),

since the C=O–Ru interaction is kept when NH_3 covers the surface (Scheme 5e). In contrast, in the case of furoin, NH_3 bridges the interaction between the OH group and the Ru(0001) surface *via* H-bonding (Scheme 5b), resulting in lower stability.

We also investigated the relative stability of the alcohol–imine and its two tautomers on Ru(0001) in the presence of adsorbed NH_3 and ad-H species. The alcohol–imine interacts preferentially with Ru(0001) *via* the NH group (Scheme 5g), but the adsorption energy is lower compared to the value on

Table 1 Survey of catalysts for the reductive amination of furoin with NH_3 and H_2[a]

Entry	Catalyst	Yield of alcohol–amine (%)
0	—	0
1	5% Pd/Al_2O_3	28
2	5% Rh/Al_2O_3	10
3	5% Pt/Al_2O_3	14
4	0.1% Ru/Al_2O_3	30
5	1% Ru/Al_2O_3	35
6	2% Ru/Al_2O_3	40
7	5% Ru/Al_2O_3 (6.7 nm[b])	40
8	5% Ru/SiO_2	35
9	5% Ru/C (2.8 nm[b])	40

[a] Reaction conditions: furoin (60 mg), NH_3 (0.45 g), % Ru/Al_2O_3 (12 mg), DMF (2 mL), 160 °C, 2 h, H_2 (2.0 MPa). The catalyst was pre-reduced at 200 °C before the reaction. [b] Average particle size of Ru nanoparticles measured by HR-TEM.
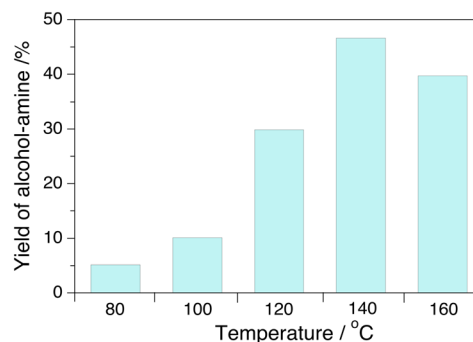

Fig. 2 Effect of temperature on furoin amination with NH_3/H_2 over 5% Ru/Al_2O_3. Reaction conditions: furoin (60 mg), NH_3 (0.45 g), 5% Ru/Al_2O_3 (12 mg), DMF (2 mL), 2 h, 2.0 MPa H_2, catalyst pre-reduced at 200 °C before the reaction. The furoin conversion was complete in all experiments. Alcohol–imine tautomers and 2,3,5,6-tetra(furan-2-yl) pyrazine were generated as the main by-products (not quantified).

Catalysis Science & Technology

Fig. 3 Effect of H_2 pressure on furoin amination with NH_3/H_2 over 5% Ru/Al$_2$O$_3$. Reaction conditions: furoin (60 mg), NH_3 (0.45 g), 5% Ru/Al$_2$O$_3$ (12 mg), DMF (2 mL), 160 °C, 2 h, catalyst pre-reduced at 200 °C before the reaction. The furoin conversion was complete in all experiments. Alcohol–imine tautomers and 2,3,5,6-tetra(furan-2-yl)pyrazine were generated as the main by-products (not quantified).
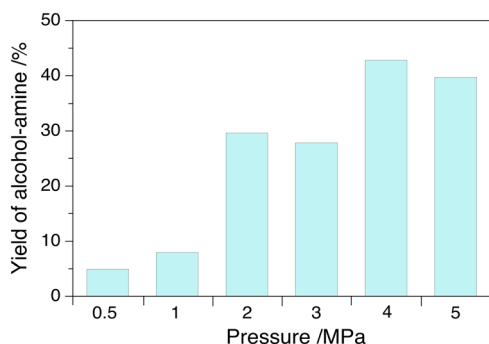
Table 2 Energy of adsorption (ΔE_{ads}, kJ mol^{-1}) of reactants, products and intermediates for the most stable configurations on bare Ru(0001) and the effect of coverage by NH_3 and ad-H

Entry	Molecule	Interacting groups	ΔE_{ads}@bare Ru(0001)	ΔE_{ads}@ad-H and NH_3 Ru(0001)
1	Furoin	C=O	−59	—
2	Furoin	OH	−37	—
3	Furoin	Furan rings	+14	—
4	Furoin	C=O + OH	−156	−74
5	Furil	C=O + C=O	−115	−107
6	Alcohol–amine	NH$_2$	−189	−36
7	Diamine	NH$_2$	−91	−24
8	Diimine	NH + NH	−252	−185
9	Alcohol–imine	NH	−92	−31
10	Alcohol enamine	NH$_2$	−45	−12
11	Keto–amine	NH$_2$	−67	−23

the bare surface (−31 vs. −92 kJ mol^{-1}, entry 9) due to steric hindrance. The alcohol–imine is −19 kJ mol^{-1} more stable than the alcohol–enamine and −8 kJ mol^{-1} more stable than the keto–amine tautomer over NH_3 and ad-H-covered Ru(0001) (entries 10–11) (see also Fig. S3†). This relative stability opposes that observed in bulk solution, where the keto–enamine is the most stable tautomer being 45 kJ mol^{-1} more stable than the alcohol–imine and 27 kJ mol^{-1} less stable than the keto–amine.

This body of results points out that the alcohol–imine is a likely intermediate responsible for the formation of the alcohol–amine over Ru(0001). The weak adsorption of the alcohol–imine and its tautomers over Ru(0001) can favor their desorption from the catalyst and the further formation of 2,3,5,6-tetra(furan-2-yl)pyrazine among other cyclic by-products in bulk solution competing with the alcohol–amine proceeding over the catalyst. Besides, preferential interaction of NH or NH$_2$ groups of the alcohol–imine and keto–amine, respectively, on Ru(0001) discourages the formation of the diimine and amine–imine intermediates, and in turn hinders diamine formation. This selectivity shortcoming has also
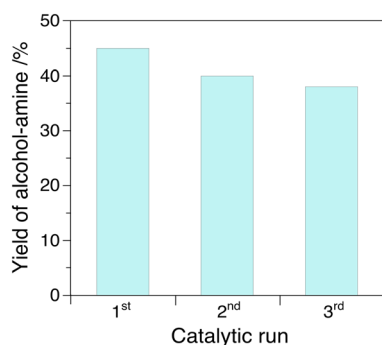
been observed in the amination of isosorbide with NH_3 and H_2, where the exo-OH group exhibits much lower reactivity than the endo-OH group, resulting in the formation of amino-alcohols with different stereochemistry as the main products with small amounts of diamines.[18]

Single-reactor tandem benzoin condensation + reductive amination process

With the results above, we investigated the credentials of a tandem reaction for the synthesis of the alcohol–amine starting from FF by combining supported bim–silica[11d] and Ru/Al$_2$O$_3$ catalysts in a single reactor (Scheme 6). In this test, both catalysts were loaded in the reactor together with DMF, FF and DBU to activate bim. First, the benzoin condensation reaction was carried out at 30 °C for 20 h. Subsequently, NH_3 and H_2 were added, and the amination reaction was carried out at 140 °C for 2 h. The results clearly show the formation of the alcohol–amine product (Fig. 5) with 42% overall yield.

Fig. 4 Catalyst recycling and reuse for experiments carried out over 5% Ru/Al$_2$O$_3$. Reaction conditions: 60 mg furoin, 0.45 g NH_3, 0.012 g 5% Ru/Al$_2$O$_3$, 2 mL DMF, 2 h, 4.0 MPa H_2, catalyst pre-reduced at 200 °C before the reaction.
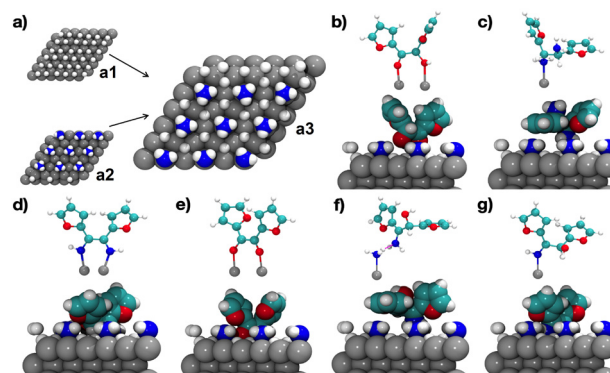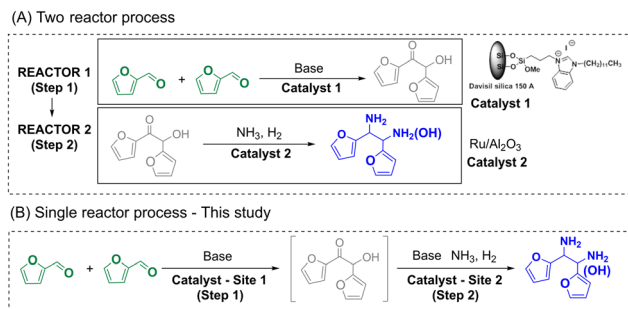

Scheme 5 (a) Single H_2 and NH_3 coverage and co-coverage on Ru(0001) (a1–a3), and most stable surface configurations for (b) furoin, (c) diamine, (d) diimine, (e) furil, (f) alcohol–amine and (g) alcohol–imine, represented both as balls-and-stick representations of the interactions.

This journal is © The Royal Society of Chemistry 2024

Catal. Sci. Technol., 2024, **14**, 2593–2599 | **2597**

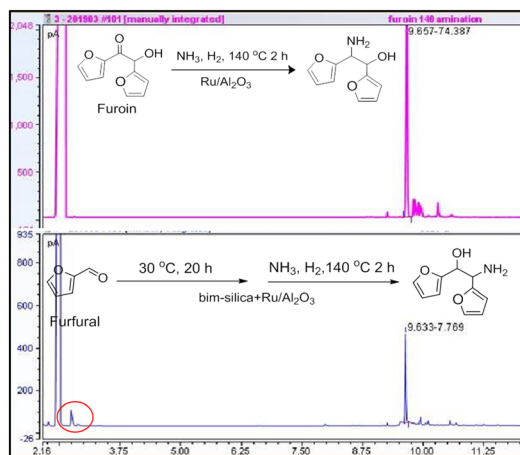**Scheme 6** Two-reactor *vs.* single reactor tandem process for the synthesis of hydrogenated derivatives from FF.

Fig. 5 Representative GC plots of the reaction system after the amination reaction of furoin with NH_3 and H_2 over (top) Ru/Al_2O_3 and (bottom) bim–silica + Ru/Al_2O_3 in the single-reactor tandem process. Reaction conditions: (top) furoin (0.12 g, 0.625 mmol), catalyst (24 mg), DMF (2 g), NH_3 (0.7 g), 140 °C, 4.0 MPa H_2, 2 h, catalyst pre-reduced at 200 °C; (bottom) (1) benzoin condensation: FF (0.096 g, 1 mmol), DBU (26 mg, 0.17 mmol), bim–silica (0.16 g), catalyst (24 mg), DMF (2 g), 30 °C, 20 h, 5% Ru/Al_2O_3 catalyst pre-reduced at 200 °C; (2) reductive amination: 0.7 g NH_3, 4.0 MPa H_2, 140 °C, 2 h.

To assess the stability of bim–silica in the presence of NH_3 and H_2, the catalyst was extracted from the reaction system after the tandem reaction, washed with HCl and DMF and retested in the benzoin condensation of FF. The catalyst was found to be fully active (see the chromatogram in Fig. S4†), pointing out that the bim moiety is not detached from the support during the tandem reaction. TG analyses on the fresh and spent bim–silica catalysts confirm the stability of bim–silica during the tandem reaction (Fig. S5†).

Conclusions

Along this study, we studied the direct/reductive amination of furoin and furil with NH_3 and H_2. Without a catalyst, furoin reacts with either NH_3 or ammonium acetate to generate 2,3,5,6-tetra(furan-2-yl)pyrazine with 39% yield. Furil also reacts with NH_3 to generate 2,2′-bipyridine-3,3′-diol with 44% yield. When Ru/Al_2O_3 and H_2 were added to the reaction

system, furoin and furil generated 2-amino-1,2-di(furan-2-yl) ethan-1-ol (alcohol–amine) as the main product with 47% and 34% yield, respectively, at 140 °C for 2 h. DFT simulations underscored the significance of the unique adsorption orientation of these intermediates on Ru/Al_2O_3, with the NH group in proximity to Ru centers and the OH group oriented away from the surface. This orientation, as revealed by our computational analysis, plays a pivotal role in guiding the reaction towards the formation of alcohol–amine, corroborating the experimentally observed product distribution. The alcohol–imine exhibits weak adsorption on ad-H/NH_3-covered Ru, allowing the formation of 2,3,5,6-tetra(furan-2-yl)pyrazine in solution competing with alcohol–amine formation on Ru. By combining Ru/Al_2O_3 and a silica-anchored N-hetero-cyclic carbene (NHC) catalyst, 2-amino-1,2-di(furan-2-yl)ethan-1-ol could be accessed with 42% overall yield in a single reactor.

Author contributions

LG: experimental data acquisition, data curation, formal analysis, writing original draft; MDP & MC: DFT calculation, data curation, formal analysis, writing original draft; FJ: investigation, formal analysis, supervision; RR: formal analysis, visualization; MPT: conceptualization, funding acquisition, resources, supervision, validation, visualization, writing – review & editing.

Conflicts of interest

There are no conflicts to declare.

Acknowledgements

References

1   (*a*) R. Mariscal, P. Maireles-Torres, M. Ojeda, I. Sádaba and M. López Granados, *Energy Environ. Sci.*, 2016, **9**, 1144; (*b*) X. Li, P. Jia and T. Wang, *ACS Catal.*, 2016, **6**, 7621; (*c*) J.-P. Lange, E. van der Heide, J. van Buijtenen and R. Price, *ChemSusChem*, 2012, **5**, 150.

2   (*a*) J. Thoen and R. Busch, Industrial Chemicals from Biomass – Industrial Concepts, in *Biorefineries-Industrial Processes and Products: Status Quo and Future Directions*, ed. B. Kamm, P. R. Gruber and M. Kamm, Wiley, 2005, ch. 12, p. 347; (*b*) G. W. Huber, J. N. Chheda, C. J. Barrett and J. A. Dumesic, *Science*, 2005, **308**, 1446; (*c*) J. Q. Bond, A. A. Upadhye, H. Olcay, G. A. Tompsett, J. Jae, R. Xing, D. M. Alonso, D. Wang, T. Zhang, R. Kumar, A. Foster, S. M. Sen, C. T. Maravelias, R. Malina, S. R. H. Barrett, R. Lobo, C. E.

2598 | *Catal. Sci. Technol.*, 2024, **14**, 2593–2599

This journal is © The Royal Society of Chemistry 2024

Wyman, J. A. Dumesic and G. W. Huber, *Energy Environ. Sci.*, 2014, **7**, 1500–1523; (*d*) M. J. Climent, A. Corma and S. Iborra, *Green Chem.*, 2014, **16**, 516; (*e*) K. Yan, G. Wu, T. Lafleur and C. Jarvis, *Renewable Sustainable Energy Rev.*, 2014, **38**, 663.

3 (*a*) Q. Girka, N. Hausser, B. Estrine, N. Hoffmann, J. Le Bras, S. Marinkovic and J. Muzart, *Green Chem.*, 2017, **19**, 4074; (*b*) M. Pelckmans, T. Renders, S. Van de Vyver and B. F. Sels, *Green Chem.*, 2017, **19**, 5303; (*c*) A. Velty, S. Iborra and A. Corma, *ChemSusChem*, 2022, **15**, e202200181.

4 (*a*) J. J. Martínez, E. Nope, H. Rojas, M. H. Brijaldo, F. Passos and G. Romanelli, *J. Mol. Catal. A: Chem.*, 2014, **392**, 235; (*b*) S. Nishimura, K. Mizuhori and K. Ebitani, *Res. Chem. Intermed.*, 2016, **42**, 19; (*c*) M. Chatterjee, T. Ishizaka and H. Kawanami, *Green Chem.*, 2016, **18**, 487; (*d*) T. Komanoya, T. Kinemura, Y. Kita, K. Kamata and M. Hara, *J. Am. Chem. Soc.*, 2017, **139**, 11493; (*e*) A. Dunbabin, F. Subrizi, J. M. Ward, T. D. Sheppard and H. C. Hailes, *Green Chem.*, 2017, **19**, 397; (*f*) J. A. T. Caetano and A. C. Fernandes, *Green Chem.*, 2018, **20**, 2494; (*g*) D. Chandra, Y. Inoue, M. Sasase, M. Kitano, A. Bhaumik, K. Kamata, H. Hosono and M. Hara, *Chem. Sci.*, 2018, **9**, 5949; (*h*) Z. Kuo, C. Bixian, Z. Xiaoting, K. Shimin, X. Yongjun and W. Jinjia, *ChemCatChem*, 2019, **11**, 5562; (*i*) D. Deng, Y. Kita, K. Kamata and M. Hara, *ACS Sustainable Chem. Eng.*, 2019, **7**, 4692; (*j*) J. He, L. Chen, S. Liu, K. Song, S. Yang and A. Riisager, *Green Chem.*, 2020, **22**, 6714; (*k*) K. Saini, S. Kumar, H. Li, S. A. Babu and S. Saravanamurugan, *ChemSusChem*, 2022, **15**, e202200107; (*l*) C. C. Truong, D. K. Mishra and Y.-W. Suh, *ChemSusChem*, 2023, **16**, e202201846.

5 S. Jiang, E. Muller, F. Jerôme, M. Pera-Titus and K. De Oliveira Vigier, *Green Chem.*, 2020, **22**, 1832.

6 (*a*) S. Jiang, C. Ma, E. Muller, M. Pera-Titus, F. Jerôme and K. De Oliveira Vigier, *ACS Catal.*, 2019, **10**, 8893; (*b*) S. Jiang, E. Muller, M. Pera-Titus, F. Jerôme and K. De Oliveira Vigier, *ChemSusChem*, 2020, **13**, 1699.

7 (*a*) D. Enders, O. Niemeier and A. Henseler, *Chem. Rev.*, 2007, **107**, 5606; (*b*) R. S. Menon, A. T. Biju and V. Nair, *Beilstein J. Org. Chem.*, 2016, **12**, 444.

8 (*a*) D. Liu, Y. Zhang and E. Y.-X. Chen, *Green Chem.*, 2012, **14**, 2738; (*b*) D. Liu and E. Y.-X. Chen, *ChemSusChem*, 2013, **6**, 2236; (*c*) H. Zang and E. Y.-X. Chen, *Int. J. Mol. Sci.*, 2016, **16**, 7143; (*d*) J. Li, B. Wang, Y. Dou and Y. Yang, *RSC Adv.*, 2019, **9**, 10825.

9 (*a*) R. Breslow, *J. Am. Chem. Soc.*, 1957, **79**, 1762; (*b*) R. Breslow, *J. Am. Chem. Soc.*, 1958, **80**, 3719.

10 (*a*) K.-I. Iwamoto, H. Kimura, M. Oike and M. Sato, *Org. Biomol. Chem.*, 2008, **6**, 912; (*b*) K.-I. Iwamoto, M. Hamaya, N. Hashimoto, H. Kimura, Y. Suzuki and M. Sato, *Tetrahedron Lett.*, 2006, **47**, 7175.

11 (*a*) L. Wang and E. Y.-X. Chen, *ACS Catal.*, 2015, **5**, 6907; (*b*) J. Wilson and E. Y.-X. Chen, *ACS Sustainable Chem. Eng.*, 2016, **4**, 4927; (*c*) E. Y.-X. Chen, L. Wang and Y. Eguchi, US0346774A1, 2016; (*d*) I. Miletto, M. Meazza, G. Paul, M. Cossi, E. Gianotti, L. Marchese, R. Rios, M. Pera-Titus and R. Raja, *Chem. – Eur. J.*, 2022, **28**, e202202771.

12 (*a*) D. Liu and E. Y.-X. Chen, *ChemSusChem*, 2013, **6**, 2236; (*b*) D. J. Liu and E. Y.-X. Chen, *ACS Catal.*, 2014, **4**, 1302; (*c*) J. Keskiväli, P. Wrigstedt, K. Lagerblom and T. Repo, *Appl. Catal., A*, 2017, **534**, 40.

13 E. Y.-X. Chen and D. Liu, US9469626B2, 2016.

14 S. Wang, Q. Gu, X. Chen, T. Zhao and Y. Zhang, *Eur. J. Chem.*, 2011, **2**, 173–177.

15 N.-T. Le, A. Byun, Y. Han, K.-I. Lee and H. Kim, *Green Sustainable Chem.*, 2015, **5**, 115–127.

16 L. R. Danielson, M. J. Dresser, E. E. Donaldson and J. T. Dickinson, *Surf. Sci.*, 1978, **71**, 599.

17 I. M. Ciobîcă, F. Frechard, R. A. van Santen, A. W. Kleyn and J. Hafner, *J. Phys. Chem. B*, 2000, **104**, 3364.

18 H. Hu, M. A. Ramzan, R. Wischert, F. Jerôme, C. Michel, K. de Oliveira Vigier and M. Pera-Titus, *ACS Sustainable Chem. Eng.*, 2023, **11**, 8229.

19 H. Mortensen, L. Diekhöner, A. Baurichter, E. Jensen and A. C. Luntz, *J. Chem. Phys.*, 2000, **113**, 6882.

20 X. Hu, M. Yang, D. Xie and H. Guo, *J. Chem. Phys.*, 2018, **149**, 044703.

21 N. Gerrits and G.-J. Kroes, *J. Phys. Chem. C*, 2019, **123**, 28291.

This journal is © The Royal Society of Chemistry 2024

Catal. Sci. Technol., 2024, **14**, 2593–2599 | **2599**